# Marked Influences on the Adenine−Cytosine Base Pairs by Electron Attachment and Ionization

**Shan Xi Tian***

*Hefei National Laboratory for Physical Sciences at Microscale, Laboratory of Bond Selective Chemistry, Department of Chemical Physics, University of Science and Technology of China, Hefei, Anhui 230026, People's Republic of China*

*Received: January 9, 2005; In Final Form: April 13, 2005*

The reverse wobble and the reverse Hoogsteen adenine−cytosine mispairs regarding their radical cations and anions are studied with the hybrid three-parameter B3LYP density functional method and 6-31+G(d), 6-311+G-(2df,2p) basis sets. Hydrogen bonding mispairs are remarkably influenced by electron attachment and ionization. Only one stronger hydrogen bond N6−H (in adenine)···N3 (in cytosine) exists in the radical pair, while the strengths of two N−H···N hydrogen bonds in the neutral pair are comparable. Geometrical coplanarity is found for the neutral and cationic pairs, in contrast to the anionic pairs in which the cytosine moiety exhibits significant deformation due to electron attachment. Dissociation energies for the neutral and radical pairs are slightly higher than those of the adenine−thymine pairs but much smaller than those of the guanine−cytosine pairs. Valence-bound anions of these two adenine−cytosine pairs are thermodynamically stable by 0.1−0.2 eV with respect to the neutral pairs. On the basis of the comparison between the experimental data of the solvated clusters and the calculated values, these two pairs can be quantitatively equivalent to the clusters in which each base is solvated by five water molecules.

## 1. Introduction

Nucleic acid bases (NABs) can be damaged by far ultraviolet ionization radiation, yielding the parent cations, the daughter fragments, and the low-kinetic-energy electrons. In particular, the fragments may be the salient result of substantial damages induced by low-energy (less than 20 eV) electrons, via electron attachment or trapping to form temporary anions.[1] The temporary anion is believed to play an essential role in DNA damage and repair.[2] During the processes of electron attachment or trapping, an extra electron may occupy one empty molecular orbital of the target molecule (usually the lowest unoccupied molecular orbital, LUMO), or it may be captured by the strong electrostatic field of the molecule (e.g., the dipole electrostatic field). The former corresponds to the so-called valence-bound (VB) anion, while the latter is named the dipole-bound (DB) anion.[3] It is clear that the molecule should have a substantial dipole moment to form the DB anion.[4] As far as the NABs (the purine and pyrimidine nucleobases), they (except for adenine) can have thermodynamically stable DB anions with respect to the neutral.[5−7] However, their VB anions are not energetically favorable.[8−11] It is interesting that the VB anions can be stabilized by the solvent water.[7,12−14] Moreover, there is overwhelming evidence that the VB anions of NABs exist in solution and the solid state. In particular, the VB anions of the Watson−Crick adenine−thymine (AT)[15] and guanine−cytosine (GC)[15−17] base pairs have been investigated, indicating a quite negative to slightly positive electron affinity (EA) for the GC pair[16,17] while a significant negative EA[15a,b] or the distinctively positive EA[15c,g] for the AT pair. Here it is noted that the second-order perturbation MP2 method is frequently hindered for the open-shell anions due to strong spin contamination.[9,12a] Density functional theory has been successfully employed in the studies of thermodynamics of the neutral, anionic, and cationic pairs.[11−18]

On the other hand, ionization radiation damage is the direct effect on the NABs. It together with electron attachment can influence the structural and energetic properties of the AT and GC pairs[15−18] and intermolecular proton-transfer processes.[15g,17,18] Although the electron attachment does not lead to ring distortion for the AT pair,[15c] the C moiety is significantly distorted in the GC anion.[16] For the AT and GC pairs, the almost positive unit is charged on the A or G moiety in the cationic pair, and the almost negative unit is charged on the T or C moiety in the anionic pair. This is consistent with the results that the vertical ionization potential ($IP_v$) of A (8.44 eV) is much smaller than the T value (9.14 eV),[19] while the vertical EA ($EA_v$) of T (−0.31 eV) is lower than the A value (−0.64 eV).[20] There are the same trends of the $IP_v$ and $EA_v$ values for G and C bases.[19,20]

As far as AC mispairing, very few studies have been reported.[21] AC mispairing may break Chargaff's rule that the amount of A or G is approximately equal to T or C, respectively. The NMR experiment showed that two possible structures involving the double hydrogen bonds (HBs) and the single HB coexist in the duplex at pH 4.5.[21] The reverse wobble (**I**) and the reverse Hoogsteen (**II**) pairing models are energetically favorable for AC base pairs (see Figures 1 and 2), where two N−H···N HBs are involved. The neutral pair **I** was predicted to be a little more stable than the pair **II**.[22] The superscript symbols (−, 0, or +) following the name indicate the overall charge state. In this work, these two pairs regarding the neutral ($AC^0$), cationic ($AC^+$), and anionic species ($AC^-$) are studied with density functional theory. The pairing geometries, vibrational frequencies, ionization potentials (IPs), EA values, pairing or dissociation energies, and interaction energies will be calculated and discussed in comparison with the related data for GC and AT pairs available in the literature.

* To whom correspondence should be addressed. E-mail: sxtian@ustc.edu.cn.

10.1021/jp050137h CCC: $30.25 
Published on Web 05/21/2005

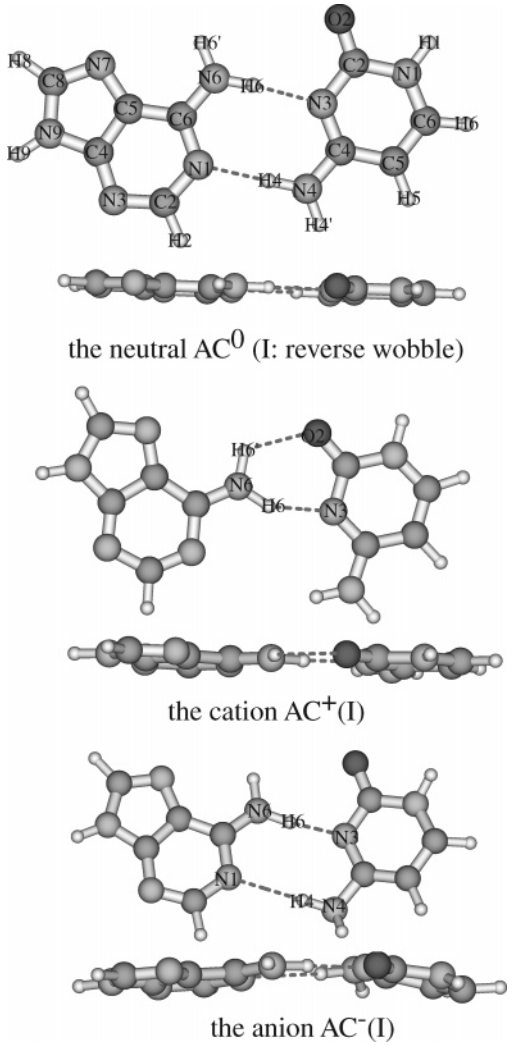


**Figure 1.** Top views and side views of the reverse wobble (**I**) AC pairs. The anion deviates visibly from planarity.

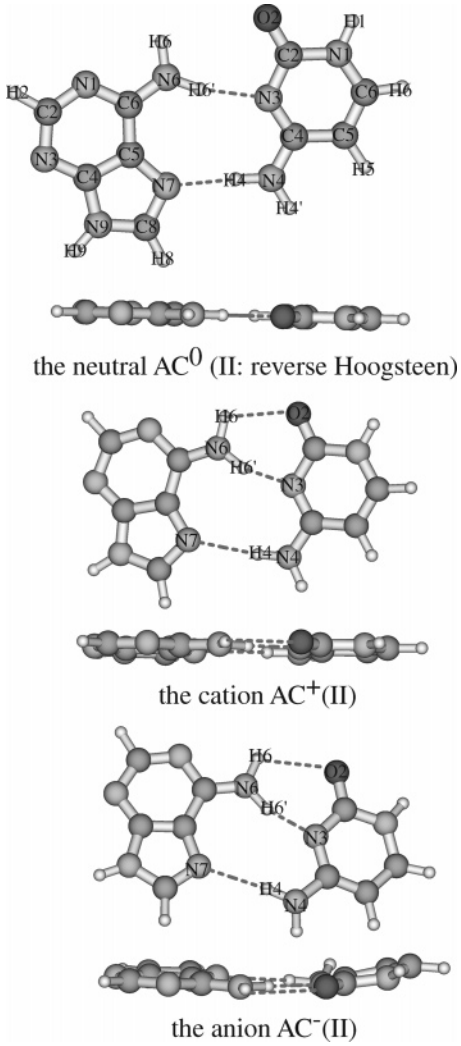


**Figure 2.** Top views and side views of the reverse Hoogsteen (**II**) AC pairs. The anion deviates visibly from planarity.

## 2. Theoretical Methods

The geometrical parameters were optimized using the hybrid density functional method B3LYP with the 6-31+G(d) basis set. This level of theory has been successfully used for the studies of NAB pairs and free bases.[17d,18] The small basis set 6-31+G(d) cannot describe the diffusely dipole-bound electron; therefore, only VB anions were studied in this work. The interaction energy, $\Delta E_{\text{int}}$, was corrected for the basis set superposition error (BSSE) using the Boys−Bernardi counterpoise (CP) scheme.[23] The basis set dependency of the energies was examined using 6-311+G(2df,2p) over the 6-31+G(d) optimized geometries and in comparison with previous theoretical results.

To elucidate the HB nature in the pairs, the electron density was calculated at the B3LYP/6-31+G(d) level and further analyzed by the natural bond orbital (NBO) program.[24] Since the occupancies of the filled NBOs are highly condensed, the delocalizing interactions can be treated by the second-perturbation energies $E(2)$

$$E(2) = -n_\sigma \frac{\langle \sigma|F|\sigma^*\rangle^2}{\epsilon_{\sigma^*} - \epsilon_\sigma} = -n_\sigma \frac{F_{ij}^{\ 2}}{\Delta\epsilon} \tag{1}$$

where $F_{ij}$ is the Fock matrix element between the NBO $i$ ($\sigma$) and $j$ ($\sigma^*$), $\epsilon_\sigma$ and $\epsilon_{\sigma^*}$ are the energies of $\sigma$ and $\sigma^*$ NBOs, and $n_\sigma$ is the population (a lone pair in the HB).[25] The interaction energy $\Delta E_{\text{int}}$ was decomposed into the charge-transfer (CT) and non-charge-transfer (NCT) parts.[25]

$$\Delta E_{\text{int}} = \Delta E_{\text{CT}} + \Delta E_{\text{NCT}} \tag{2}$$

The $\Delta E_{\text{CT}}$ term was obtained by summarizing the components of $E(2)$ for the intermolecular $n \rightarrow \sigma^*$ interactions in the HB system, as the lowering energy due to expanding the variational space on each monomer to include unfilled orbitals on the other monomer. The $\Delta E_{\text{NCT}}$ term was due to exclusive repulsion and electrostatic (induction and polarization) interactions. Recently, the NBO analysis using the DFT wave functions was successfully applied in the HB studies of our group.[26] Above calculations were carried out using the Gaussian 98 suit programs.[27]

The covalent adiabatic and vertical IPs ($IP_a$ and $IP_v$) and EAs ($EA_a$ and $EA_v$) were calculated as the difference between the absolute energies of the neutral and cation/anion species at their respective optimized (for the adiabatic values) or the neutral (for the vertical values) geometries.

$$\begin{aligned} IP_a &= E_{\text{neut}}(AC^0) - E_{\text{cation}}(AC^+) \\ IP_v &= E_{\text{neut}}(AC^0) - E_{\text{cation}}(AC^0) \end{aligned} \tag{3}$$

$$\mathrm{EA_a} = E_{\mathrm{neut}}(\mathrm{AC}^0) - E_{\mathrm{anion}}(\mathrm{AC}^-)$$
$$\mathrm{EA_v} = E_{\mathrm{neut}}(\mathrm{AC}^0) - E_{\mathrm{anion}}(\mathrm{AC}^0) \quad (4)$$

Moreover, the vertical electron detachment energies (VDE) for the anions were calculated because this value can be obtained in the anion photodetachment spectroscopy experiments.

$$\mathrm{VDE} = E_{\mathrm{neut}}(\mathrm{AC}^-) - E_{\mathrm{anion}}(\mathrm{AC}^-) \quad (5)$$

The values for the free monomers were calculated in a similar way.

### 3. Results and Discussion

**A. Hydrogen Bonding.** As shown in Figures 1 and 2, two HBs are exhibited in the pairs $AC^0$(**I**), $AC^+$(**I**), $AC^-$(**I**), and $AC^0$(**II**), while three HBs are suspected to exist in the radical pairs $AC^+$(**II**) and $AC^-$(**II**). The difference of the HBs between the neutral pair **I** and **II** is the eight-numbered ring in the former and a nine-numbered ring in the latter. Moreover, the HB lengths listed in Table 1 suggest that the HB energies of the latter should be a little higher than those of the former. The details about the HB energies will be discussed in the following text. In the cationic pair $AC^+$(**I**), a new HB N6−H6′···O2 bond is formed, while the N4−H4···N1 bond is broken. The N6−H6···N3 bond is strengthened significantly, with a distinct shortening of 0.1 Å. In contrast to the $AC^+$(**I**), the N4−H4···N1 bond is kept in $AC^-$(**I**) but weakened significantly by an elongation of 0.5 Å with respect to that in $AC^0$(**I**). Moreover, the N6−H6···N3 bond is further strengthened to the length 1.730 Å in $AC^-$(**I**). It is interesting that the HBs are influenced significantly in $AC^+$(**II**) and $AC^-$(**II**) pairs. Namely, N4−H4···N7 bonds are remarkably weakened, but new N6−H6···O2 bonds are formed. The N6−H6′···N3 bond in $AC^+$(**II**) is the shortest one among these three HBs, which is even slightly shorter than the N6−H6···N3 bond in $AC^-$(**I**). The shortening of the N6−H6-(H6′)···N3 was proposed to be a potential reason for the strong distortion of $AC^+$ away from the structure of the neutral $AC^0$, which is similar to the case of the AT pair pointed out by Hutter and Clark.[18] The (G) N−H···N (C) bond was also predicted to be shortened both in $GC^-$[16] and $GC^+$[18] with respect to the $GC^0$, respectively. Besides the HB changes in these pairs, the distinct deformation is the non-coplanarity of $AC^-$ pairs. The dihedral angle between A and C moieties in the anionic pair is about ±15°. The pyramidalization of N4 in the C moiety is shown when the extra electron attaches to the pair, which is interpreted by the traditional argument that a nitrogen atom becomes more nearly $sp^3$ hybridized and more pyramidal when it gains charge and it becomes more $sp^2$ hybridized and more planar.[16] The other changes will be further explained by the natural population (NPA) analyses[25b,25c] in section C. The intramolecular geometrical changes in the A and C moieties with respect to the free monomers are due to the intermolecular hydrogen-bonding interactions, which is not further presented in detail.

**TABLE 1: Hydrogen Bond Lengths (in Å) and Angles (in Degrees)**

| geometrical parameters | AC(**I**) | | | AC(**II**) | | |
|---|---|---|---|---|---|---|
| | $AC^0$(**I**) | $AC^+$(**I**) | $AC^-$(**I**) | $AC^0$(**II**) | $AC^+$(**II**) | $AC^-$(**II**) |
| R[(A)N1···H4(C)] | 1.982 | | 2.375 | | | |
| R[(A)H6···O2(C)] | | | | | 2.405 | 2.600 |
| R[(A)H6′···O2(C)] | | 2.162 | | | | |
| R[(A)H6···N3(C)] | 1.973 | 1.862 | 1.730 | | | |
| R[(A)H6′···N3(C)] | | | | 1.994 | 1.718 | 1.804 |
| R[(A)N7···H4(C)] | | | | 1.998 | 2.329 | 2.328 |
| A[N1···H4N4] | 178.7 | | 176.1 | | | |
| A[N6H6···N3] | 175.2 | 151.4 | 173.9 | | | |
| A[N6H6′···N3] | | | | 167.8 | 161.0 | 160.6 |
| A[N6H6···O2] | | | | | 105.2 | 105.4 |
| A[N6H6′···O2] | | 114.4 | | | | |
| A[N7···H4N4] | | | | 176.5 | 173.3 | 172.7 |

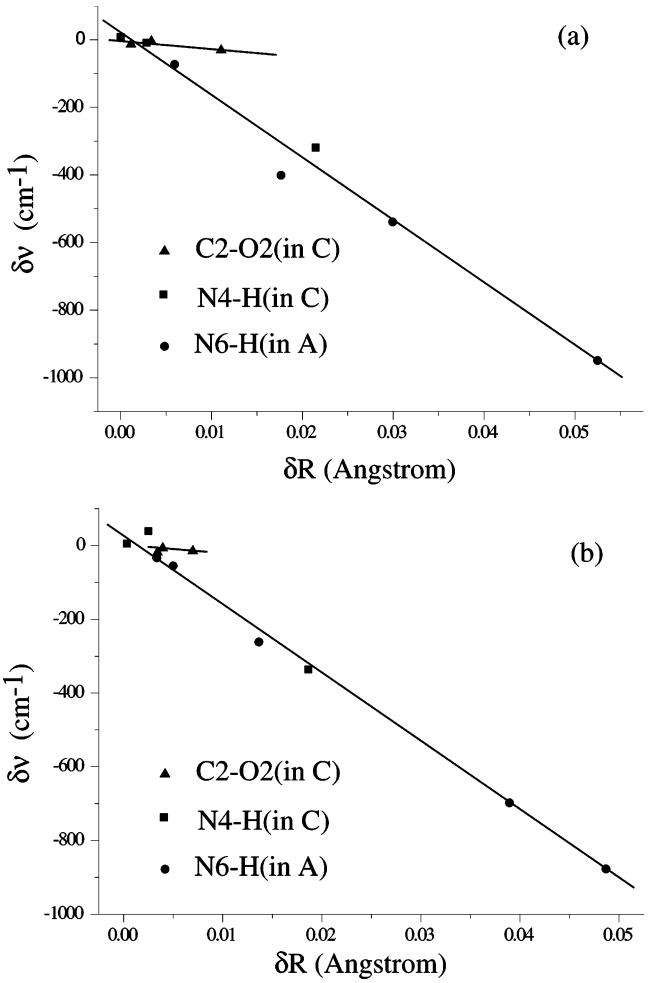


**Figure 3.** The linear correlation between bond elongation and stretching vibrational frequency shifts (a) in $AC^0$(**I**), $AC^+$(**I**), and $AC^-$(**I**); (b) in $AC^0$(**II**), $AC^+$(**II**), and $AC^-$(**II**).

It is noted that the significant elongations of the lengths of the N−H and C═O bonds in A or C due to the hydrogen bonding are in a linear correlation with the read frequency shifts of the stretching mode as shown in Figure 3. The largest red shifts are −949.55 and −877.55 $cm^{-1}$ of the N6−H6(H6′) stretching in $AC^-$(**I**) and $AC^+$(**II**), respectively. In the neutral $AC^0$(**I**), the intermediate red shifts −319.24 $cm^{-1}$ of the N4−H4 stretching and −401.21 $cm^{-1}$ of the N6−H6 stretching are predicted, and the corresponding two points in Figure 3a deviate from the fitted line. This can be interpreted by their coupling vibrations; similar phenomena have been predicted for the mixed O−H stretching in the hydrogen-bonding complexes.[26] The smaller elongations are predicted for the C═O bonds, corresponding to the smaller red shifts of the stretching vibrational frequencies.

The NBO analysis is a powerful technique for studying hybridization and covalency effects in polyatomic wave functions.[25] In the present case, the O atom involved in hydrogen bonding is mainly of p characteristics, which has the bigger $E(2)$ value with respect to the sp one. The N atom only exhibits the p characteristics in hydrogen bonding. In general, the $E(2)$ values listed in Table 2 suggest that the N6−H6(H6′)···N3

**TABLE 2: Natural Bond Orbital Analysis of Intermolecular Hydrogen Bonds**

| | | $E(2)$ (kcal/mol) | $\delta\epsilon$ (au) | $F_{ij}$ (au) |
|---|---|---|---|---|
| $AC^0$(**I**) | (A)$n_{N1} \rightarrow \sigma^*_{N4H4}$(C) | 17.86 | 0.81 | 0.109 |
| | (C)$n_{N3} \rightarrow \sigma^*_{N6H6}$(A) | 17.14 | 0.83 | 0.109 |
| $AC^+$(**I**) | (C)$n_{N3} \rightarrow \sigma^*_{N6H6}$(A) | 11.89 | 0.75 | 0.121 |
| | (C)$n_{O2} \rightarrow \sigma^*_{N6H6'}$(A)[a] | 1.26 | 0.65 | 0.037 |
| $AC^-$(**I**) | (A)$n_{N1} \rightarrow \sigma^*_{N4H4}$(C) | 2.47 | 0.86 | 0.059 |
| | (C)$n_{N3} \rightarrow \sigma^*_{N6H6}$(A) | 19.53 | 0.76 | 0.157 |
| $AC^0$(**II**) | (A)$n_{N7} \rightarrow \sigma^*_{N4H4}$(C) | 16.57 | 0.85 | 0.107 |
| | (C)$n_{N3} \rightarrow \sigma^*_{N6H6'}$(A) | 15.46 | 0.84 | 0.104 |
| $AC^+$(**II**) | (A)$n_{N7} \rightarrow \sigma^*_{N4H4}$(C) | 2.76 | 0.90 | 0.064 |
| | (C)$n_{N3} \rightarrow \sigma^*_{N6H6'}$(A) | 19.67 | 0.74 | 0.154 |
| | (C)$n_{O2} \rightarrow \sigma^*_{N6H6}$(A)[a] | 0.49 | 0.63 | 0.023 |
| $AC^-$(**II**) | (A)$n_{N7} \rightarrow \sigma^*_{N4H4}$(C) | 2.72 | 0.91 | 0.064 |
| | (C)$n_{N3} \rightarrow \sigma^*_{N6H6'}$(A) | 14.94 | 0.78 | 0.138 |
| | (C)$n_{O2} \rightarrow \sigma^*_{N6H6}$(A)[a] | 0.30 | 0.66 | 0.018 |

[a] The p branch of O2 atom is larger than the sp branch.

**TABLE 3: Charge-Transfer Energies ($\Delta E_{CT}$), Non-Charge-Transfer Energies ($\Delta E_{NCT}$), Interaction Energies ($\Delta E_{int}$) of AC Pairs (in kcal/mol)**

| | $\Delta E_{CT}$[a] | $\Delta E_{NCT}$[b] | $\Delta E_{int}$[c] |
|---|---|---|---|
| $AC^0$(**I**) | 35.00 | 20.86 | −14.14 |
| $AC^+$(**I**) | 14.15 | −15.52 | −29.67 |
| $AC^-$(**I**) | 22.00 | 1.09 | −20.91 |
| $AC^0$(**II**) | 32.03 | 18.37 | −13.66 |
| $AC^+$(**II**) | 23.27 | −7.11 | −30.38 |
| $AC^-$(**II**) | 18.12 | −3.36 | −21.48 |

[a] Sum of the $E(2)$ values of all $n_{N(O)} \rightarrow \sigma^*_{NH}$ energies. [b] $\Delta E_{NCT} = \Delta E_{int} - \Delta E_{CT}$. [c] The base-set superposition errors are corrected by the standard counterpoise method.

**TABLE 4: Intermolecular Harmonic Vibrational Frequencies (in $cm^{-1}$) in AC Pairs[a]**

| | $\omega$1 | $\omega$2 | $\omega$3 | $\omega$4 | $\omega$5 | $\omega$6 |
|---|---|---|---|---|---|---|
| AC(**I**) | | | | | | |
| $AC^0$(**I**) | 26.44 | 29.67 | 60.68 | 64.36 | 83.11 | 118.80 |
| $AC^+$(**I**) | 23.61 | 31.80 | 65.46 | 10.13 | 88.62 | 134.36 |
| $AC^-$(**I**) | 22.95 | 30.92 | 64.86 | 41.54 | 88.13 | 108.79 |
| AC(**II**) | | | | | | |
| $AC^0$(**II**) | 27.95 | 28.25 | 64.82 | 70.27 | 87.44 | 118.8 |
| $AC^+$(**II**) | 26.50 | 35.80 | 82.36 | 52.74 | 104.9 | 132.8 |
| $AC^-$(**II**) | 25.06 | 32.03 | 67.72 | 55.42 | 89.12 | 124.3 |

[a] $\omega$1: butterfly; $\omega$2: torsion; $\omega$3: waving; $\omega$4: in-plane bending; $\omega$5: in-plane staggering; $\omega$6: approaching.

bonds are the strongest HBs, which is consistent with the conclusion derived on the basis of the HB lengths in Table 1. The N6−H6(H6′)···N3 bond in $AC^-$(**I**) or $AC^+$(**II**) has the larger Fock matrix $F_{ij}$ (0.157 or 0.154 au) and the largest $E(2)$ values (19.53 or 19.67 kcal/mol), showing the strongest HB and the biggest electron density overlap along the hydrogen bonding direction. The distinctly smaller $F_{ij}$ and $E(2)$ values for the N6−H6···O2 bonds in $AC^+$(**II**) and $AC^-$(**II**) show that these two HBs are extremely weak, in agreement with the prediction of the longer HB lengths 2.405 and 2.600 Å in Table 1.

In Table 3 summarizes the $\Delta E_{CT}$, $\Delta E_{NCT}$, and $\Delta E_{int}$ values. $AC^0$(**I**) and $AC^0$(**II**) have the largest $\Delta E_{CT}$ energies but the smallest $\Delta E_{int}$ energies due to the larger positive $\Delta E_{NCT}$ energies. The interaction energies $\Delta E_{int}$, −14.14 and −13.66 kcal/mol, are well comparable to the values predicted at the higher level of theory.[22] The smaller positive (even negative) $\Delta E_{NCT}$ energies are predicted for the radical pairs, indicating the more attractive interactions besides hydrogen bonding when the pairs are ionized or attached with the extra electron.

**B. Vibrational Frequencies and Pairing Energies.** The intermolecular harmonic vibrational frequencies are listed in Table 4. A new set of assignments has been made for these six lowest vibrational frequencies, differing from the AT or GC cases.[15c,15f,16] No distinct variances of the frequency exist between the neutral and the radical AT and GC pairs.[15c,15f,16] However, the waving $\omega$3, the in-plane bending $\omega$4, and the in-plane staggering $\omega$5 show significant frequency differences between the neutral and the radical AC pairs. This further suggests that the potential energy surfaces are dramatically changed when the pairs are charged, and the pairing geometrical changes have been shown in Figures 1 and 2.

In addition to frequency changes occurring on these pairs, the dissociation or pairing energies provide a quantitative measure of the thermodynamic stability. Since ionization and electron attachment occur on A and C moieties, respectively (as discussed in section **C**), Table 5 provides the dissociation energies of $AC^0$, $AC^+$, and $AC^-$ that are calculated for the processes of the pairs dissociated to the free monomers (including $AC^- \rightarrow A^0 + C^0 + e^-$). $AC^0 \rightarrow A^0 + C^0$ is predicted to be the most energetically favorable, while $AC^+ \rightarrow A^+ + C^0$ is the most endothermic for both the reverse wobble and the reverse Hoogsteen pairs. The B3LYP/6-311++G(2df,2p)//B3LYP/6-31+G(d) calculations give a stability of 13.29 kcal/mol for $AC^0$(**I**), 27.60 kcal/mol for $AC^+$(**I**), 18.53 kcal/mol for $AC^-$(**I**), 12.73 kcal/mol for $AC^0$(**II**), 27.78 kcal/mol for $AC^+$(**II**), and 19.06 kcal/mol for $AC^-$(**II**). It is interesting to compare the values for AT and GC pairs available in the literature.[15c,15g,16,28] Li et al. performed the calculations at the same level of theory (B3LYP/6-31+G(d)) for the GC and AT systems,[15c,15g] and they obtained results close to the B3LYP/TZ2P++ results.[16] In particular, the dissociation ener-

**TABLE 5: Dissociation Energies (in kcal/mol) for the Neutral, Cationic, and Anionic AC Pairs[a] in Comparison to GC and AT Pairs**

| | $AC^0 \rightarrow A^0 + C^0$ | $AC^+ \rightarrow A^+ + C^0$ | $AC^- \rightarrow A^0 + C^-$ | $AC^- \rightarrow A^0 + C^0 + e^-$ |
|---|---|---|---|---|
| AC(**I**) | | | | |
| B3LYP/6-31+G(d) | −13.92 (−12.26) | −28.52 (−27.57) | −18.81 (−15.06) | −15.13 (−16.84) |
| B3LYP/6-311++(2df,2p)[b] | −13.29 | −27.60 | −18.53 | −14.57 |
| AC(**II**) | | | | |
| B3LYP/6-31+G(d) | −13.43 (−11.75) | −28.80 (−27.72) | −19.61 (−15.59) | −15.92 (−17.37) |
| B3LYP/6-311++(2df,2p)[b] | −12.73 | −27.78 | −19.06 | −15.10 |
| GC | $GC^0 \rightarrow G° + C^0$ | $GC^+ \rightarrow G^+ + C^0$ | $GC^- \rightarrow G° + C^-$ | $GC^- \rightarrow G° + C^0 + e^-$ |
| | −22.9[c] | −40.5[c] | −36.2[c] | |
| | −23.9,[d] −21.0[f] | | −35.6[d] | −33.4[d] |
| AT | $AT^0 \rightarrow A^0 + T^0$ | $AT^+ \rightarrow A^+ + T^0$ | $AT^- \rightarrow A^0 + T^-$ | $AT^- \rightarrow A^0 + T^0 + e^-$ |
| | −10.7[c] | −20.6[c] | −12.8[c] | |
| | −11.9,[e] −13.0[f] | | −14.8[e] | −15.3[e] |

[a] Zero-point corrected dissociation energies are given in the parentheses. [b] Over the B3LYP/6-31+G(d) geometries. [c] The B3LYP/6-31+G(d) results from ref 15g. [d] The B3LYP/TZ2P++ results from ref 16. [e] The B3LYP/TZ2P++ results from ref 15c. [f] The experimental data from ref 28.

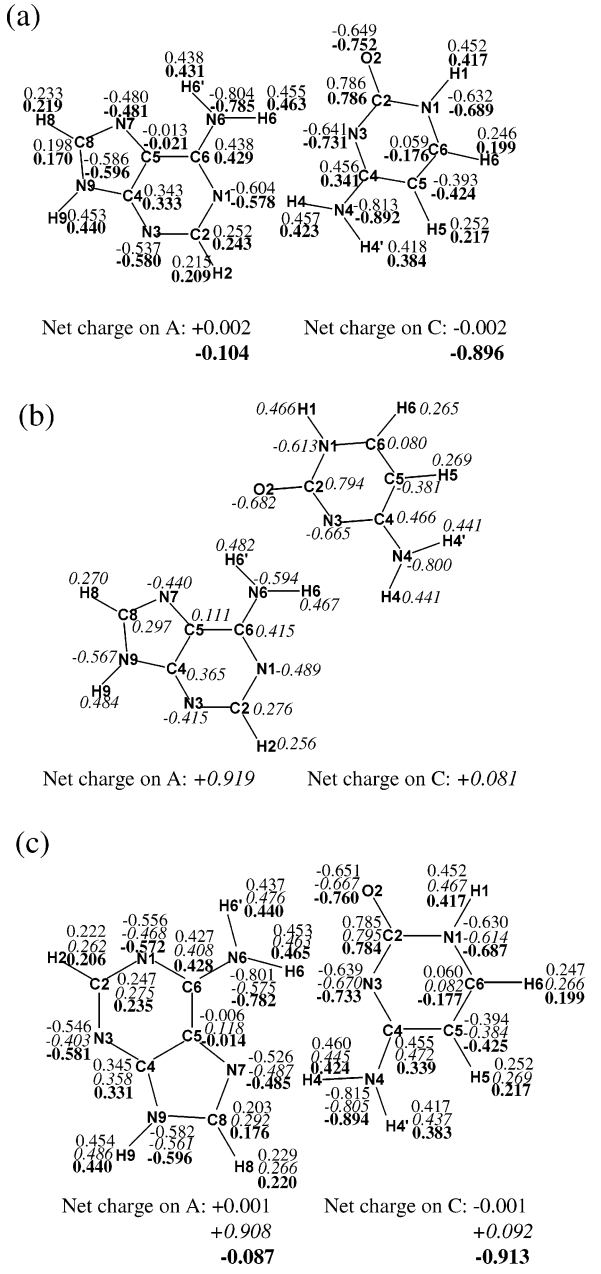


**Figure 4.** Natural population (NPA) charges on each atom in the neutral (normal), cationic (italic), and anionic (bold) AC pairs. (a) and (b) for AC(**I**) pairs; (c) for AC(**II**) pairs.

gies of $AT^0$ and $GC^0$ [15c,15g] are in good agreement with the experimental data.[28] The comparison in Table 5 indicates that the thermodynamic stability for the AC system is slightly higher than that of the AT system but much lower than that of the GC system.[15c,15g,16,28]

**C. Natural Population Charge Analysis.** Figure 4 shows the NPA charge distributions for the neutral, cationic, and anionic pairs. Almost no net charge is on each moiety in the $AC^0$ pairs, in contrast to the $AT^0$ (−0.02 on T and 0.02 on A)[15c] and $GC^0$ (−0.36 on G and 0.36 on C)[16] pairs. As expected, the cationic charges lie mostly on A moiety, which takes 0.919 in $AC^+$(**I**) or 0.908 in $AC^+$(**II**), due to the lower $IP_v$ of A with respect to C.[19] The dramatic decrease of electronic charge at the N1 atom or N7 atom leads to weakening of the N4−H4···N1(N7) bond in the cationic pair. In particular, the charge on the N1 atom in $AC^0$(**I**) decreases from −0.604 to −0.489 in $AC^+$(**I**), while the charge increase on H6′ (in A) and O2 (in C) atoms leads to the formation of N6−H6′···O2 in $AC^+$(**I**). The charge decrease on N6 atom strengthens the N6−H6′···O2 and N6−H6···N3 bonds in $AC^+$(**I**) via an elongation of the N6−H6(H6′) bond. The anionic charges lie mostly on C, which takes −0.896 in $AC^-$(**I**) or −0.913 in $AC^-$(**II**) of the extra electronic unit charge. The atoms N3, O2, and N4 show the greatest charge shifts. They strongly attract the positive-charged H6(H6′) atom; in particular, the N6−H6···N3 bond is strengthened significantly in the AC(**II**) radical pairs with respect to the neutral pairs.

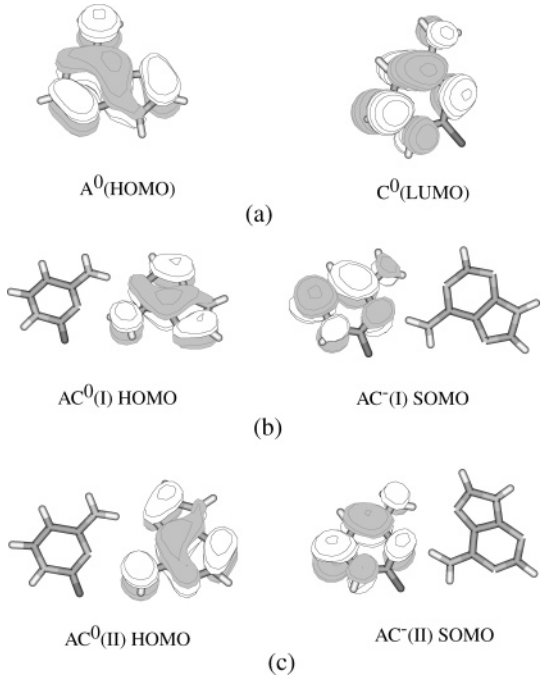


**Figure 5.** Molecular orbitals involved in AC cation and anion formation. The HOMO of A is similar to the HOMO of AC pairs, revealing that the lowest ionization states correspond to ionization on the A moiety in the pairs. The LUMO of C is similar to AC anion SOMOs, indicating that the extra electron lies predominately on the C moiety and the AC anions are at the valence-bound state.

In Figure 5, the B3LYP/6-31+G(d) orbital plots for the highest occupied molecular orbital (HOMO) of $A^0$, the LUMO of $C^0$, HOMOs of $AC^0$(**I**) and $AC^0$(**II**), and the single occupied molecular orbitals (SOMOs) of $AC^-$(**I**) and $AC^-$(**II**) are shown. It is clear that the lowest ionized state of the AC pair corresponds to ionization on the A moiety, while the $AC^-$ pairs are the VB anions in which the extra electron occupies on the LUMO of $C^0$. It is noted that the neutral AC pairs have the larger dipole moments (ca. 4.5 D for **I** and ca. 9.4 D for **II**), exhibiting the possibility of the existence of the DB anions. We only focus on the VB anionic states of the AC pairs in this work.

**D. Electron Affinities and Ionization Potentials.** The photoelectron spectroscopy studies have demonstrated that the naked nucleobase VB anions are not thermodynamically stable or short-lived.[3,6,7,13,14] Microsolvation with even a single water molecule provides sufficient stabilization to facilitate electron binding for uracil, thymine, and cytosine.[5,6,12−14] On the other hand, the DB anionic states of uracil, thymine, and cytosine have been detected and theoretically investigated.[6−9,13,14] In particular, the VDE of the DB cytosine anionic state was measured at 0.085 ± 0.008 eV.[7] The $EA_a$ and $EA_v$ values corresponding to their VB anionic states are proposed to be negative both from the experiments and the theoretical calculations. On the other hand, the $IP_v$ values of the nucleobases solvated with the water molecules were studied experimentally

**TABLE 6: Vertical and Adiabatic Electron Affinities ($EA_v$, $EA_a$), Ionization Potential ($IP_v$, $IP_a$), and Vertical Detachment Energies (VDE) for A, C, and AC Pairs (in eV)[a] Together with the GC and AT Species for Comparison**

| | $EA_v$ | $EA_a$ | $IP_v$ | $IP_a$ | VDE |
|---|---|---|---|---|---|
| A | | | 8.25 | 8.06 | |
| | −0.64[b] | −0.045[c] | 8.29, (8.44, 8.45)[g] | 8.07, 8.26,[j] 7.80[k] | |
| C | −0.63 | −0.39 | | | |
| | −0.54, −0.36[b] | −0.17 | 8.94[h] | 8.68,[j] 8.45[k] | 0.085[h] |
| AC(**I**) | −0.26 | 0.20 | 7.68 | 7.40 | 0.81 |
| | −0.17 | 0.06 | 7.72 | 7.45 | 0.88 |
| AC(**II**) | −0.23 | 0.24 | 7.63 | 7.37 | 0.84 |
| | −0.14 | 0.10 | 7.67 | 7.42 | 0.91 |
| GC | −0.15 | 0.48[d], 0.49[i] | 7.23[i] | 6.90[i] | 1.16[i] |
| AT | −0.16 | −0.40,[e] 0.31[f], 0.30[i] | 7.80 | 7.68 | 0.60 |

[a] The values at the upper line calculated at the B3LYP/6-31+G(d) level; the below ones calculated at the B3LYP/6-311+G(2df,2p)//B3LYP/6-31+G(d) level. [b] Mean value taken from refs 3 and 8 (discrepancies 0.02−0.20 eV). [c] The experimental data from ref 14c. [d] The B3LYP/TZ2P++ results from ref 16. [e] Ref 15b. [f] The B3LYP/TZ2P++ results from ref 15c. [g] The experimental data from ref 19a,b. [h] Of the dipole-bound anion.[7] [i] The B3LYP/6-31+G(d) results from refs 15g and 17. [j] From ref 19c. [k] From ref 19d.

and found to decrease with the increase of the number of the solvent water molecules.[19a] Here it is noted that the high temperature to heat the solid sample in the experiments[7,19a] may lead to more tautomers or the vibrational excited states that correspond to the different VDEs or $IP_v$ values. However, Schiedt et al. thought the hot anions had been cooled after traveling through a long distance for the mass selection, and thereby they obtained information of different forms of electron binding in the mass-selected and cooled nucleobases uracil, thymine, and cytosine and their water clusters.[7] It is feasible that ab initio results corresponding to the most stable species compare directly with the experimental data.[7,19a]

The $EA_v$, $EA_a$ of C and the $AC^0$ pairs, $IP_v$ and $IP_a$ of A and the $AC^0$ pairs, and VDE of the $AC^-$ pairs are listed in Table 6, together with the related data of the GC and AT pairs.[15b,15c,15g,16,17] The present calculations indicate that the $AC^-$ anionic pairs are more stable with 0.1−0.2 eV than the neutral $AC^0$ pairs. The VDEs of the former are 0.8−0.9 eV. However, the vertical electron attachment to the $AC^0$ pair is endothermic. The geometrical relaxation as well as the intermolecular interactions plays a key role to trap the extra electron in the pairs. The $IP_v$ values of the $AC^0$ pairs are predicted to be 7.6−7.7 eV, and they are much smaller than the $A^0$ value.[19] According to the NBO theorem, the orbital interactions via hydrogen bonding leads to the strong mixture between the occupied and unoccupied orbitals.[25] It enhances the energy level of the HOMO of the pair, correspondingly showing the lower $IP_v$ with respect to the free monomer. In general, these values for the AC pairs are closer to the AT pairs'. For the GC and AT pairs, the $EA_a$ values calculated at the B3LYP/6-31+G(d) level[15g,17] are found to be extremely close to the B3LYP/TZ2P++ results,[15c,16] which together with comparison between the present calculated results and the experimental data demonstrates the reliability of the B3LYP/6-31+G(d) level of theory.

A comparison of the VDEs between the solvated cytosine $C(H_2O)_n^-$[7] and the $AC^-$ pairs is shown in Figure 6a. Although the thermally stable $C^-$ in the experiment[7] is the DB anion, its VDE is in a good linear correlation with the number ($n$) of the solvent water molecules

$$\mathrm{VDE} = -0.08267 + 0.19029n \qquad (6)$$

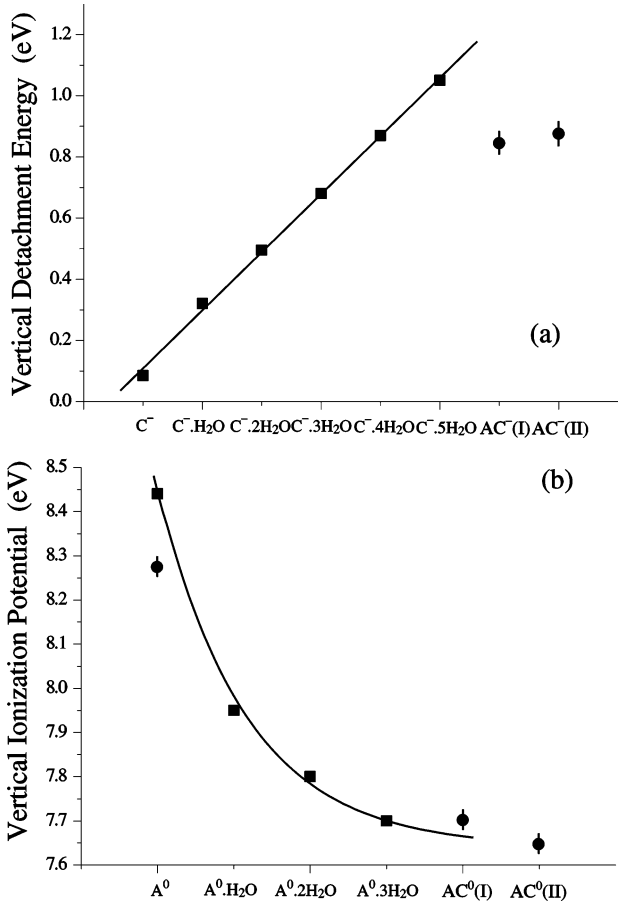


**Figure 6.** Comparison of (a) the vertical detachment energy (VDE) of the microsolvated C (from ref 7) and the VDEs for $AC^-$ pairs in (a); and (b) the vertical ionization potentials ($IP_v$) of the microsolvated A (from ref 19a) and $IP_v$ values of $AC^0$ pairs. The calculated values (solid circle) are the mean between the B3LYP/6-31+G(d) and B3LYP/6-311++G(2df,2p) data, and the derivates are the difference between these two calculated data.

where the correlation parameter $r \sim 0.9991$. The VDEs of the $AC^-$ pairs correspond to $n \sim 5$. The experimental $IP_v$ values of $A(H_2O)_n$[19a] decrease with the increase of water number $n$, which is fitted by an exponent function,

$$\mathrm{IP_v} = 7.67 + 0.768\exp(-n/1.027) \qquad (7)$$

where the parameter $r \sim 0.9999$. Although the calculated $IP_v(A^0)$ is a little lower than the experimental datum, the $IP_v$ of the $AC^0$ pairs are still used to estimate the microsolvation effect of C to A. The mean $n$ value is estimated to be ca. 5. Namely, the microsolvation of C to A in the pairs is also quantitatively equivalent to five water molecules.

## 4. Concluding Remarks

The hybrid density functional B3LYP with 6-31+G(d) and 6-311+G(2df,2p) basis sets is used to calculate the geometrical, vibrational, and energetic properties of the mispairs AC regarding the neutral, cationic, and anionic species. Hydrogen bonding mispairs are remarkably influenced by electron attachment and ionization. Only one stronger N6−H(A)···N3(C) hydrogen bond exists in the radical pairs, while the strengths of two hydrogen bonds N−H···N in the neutral pair are comparable. Moreover, the geometrical coplanarity is found for the neutral and cationic pairs, in contrast to the anionic pairs in which the cytosine moiety exhibits significant geometrical deformation due to the

extra electron attachment. The AC pairs are predicted to have the positive $EA_a$ values of 0.1−0.2 eV. The thermodynamic stabilities are also enhanced for the cationic pairs with respect to the neutral ones, which is similar to AT and GC pairs and more similar to AT.[15−17] The analogy of VED and $IP_v$ values to microsolvation demonstrates that A solvates C or C solvates A as about five solvent water molecules, on the basis of comparison to the experimental microsolvation data that show the increase in VED[7] or the decrease in $IP_v$[19a] with respect to the free monomer.

**Acknowledgment.** This work is supported by the fund for the young research fellows at University of Science and Technology of China.

## References and Notes

(1) (a) *Radiation Damage in DNA: Structure/Function Relationships at Early Times*; Fuciarelli, A. F.; Zimbrick, J. D. Eds.; Battelle: Columbus, OH, 1995. (b) von Sonntag, C. *The Chemical Basis of Radiation Biology*; Taylor and Francis: London, 1987. (c) Dandliker, P. J.; Holmlin, R. E.; Barton, J. K. *Science* **1997**, *275*, 1465.

(2) (a) Boudaiffa, B.; Cloutier, P.; Hunting, D.; Huels, M. A. Sanche, L. *Science* **2000**, *287*, 1658. (b) Gajewski, E.; Dizdaroglu, M. *Biochemistry* **1990**, *29*, 977. (c) Colson, A. O.; Sevilla, M. D. *Int. J. Radiat. Biol.* **1995**, *67*, 627. (d) Denifl, S.; Ptasinska, S.; Hanel, G.; Gstir, B.; Probst, M.; Scheier, P.; Mark, T. D. *J. Chem. Phys.* **2004**, *120*, 6557.

(3) Aflatooni, K.; Gallup, G. A.; Burrow, P. D. *J. Phys. Chem. A* **1998**, *102*, 6205.

(4) (a) Fermi, E.; Teller, E. *Phys. Rev.* **1947**, *72*, 399. (b) Wightman, A. S. *Phys. Rev.* **1950**, *77*, 521.

(5) (a) Olyer, N. A.; Adamowicz, L. *J. Phys. Chem.* **1993**, *97*, 11122. (b) Roerig, G. H.; Olyer, N. A.; Adamowicz, L. *J. Phys. Chem.* **1995**, *99*, 14285. (c) Olyer, N. A.; Adamowicz, L. *Chem. Phys. Lett.* **1994**, *219*, 223.

(6) (a) Hendricks, J. H.; Lyapustina, S. A.; de Clercq, H. L.; Snodgrass, J. T.; Bowen. K. H. *J. Chem.* Phys. **1996**, *104*, 7788. (b) Desfrancois, C.; Abdoul-Carime, H.; Schermann, J. P. *J. Chem. Phys.* **1996**, *104*, 7792. (c) Desfrancois, C.; Abdoul-Carime, H.; Carles, S.; Periquet, V.; Schermann, J. P.; Smith, D. M. A.; Jolbout, A. F.; Smets, J.; Adamowicz, L. *J. Chem. Phys.* **1999**, *110*, 11876.

(7) Schiedt, J.; Weinkauf, R.; Neumark, D. M.; Schlag, E. W. *Chem. Phys.* **1998**, *239*, 511, and references therein.

(8) Sevilla, M. D.; Besler, B.; Colson, A. O. *J. Phys. Chem.* **1995**, *99*, 1060.

(9) Dolgounitcheva, O.; Zakrzewski, V. G.; Ortiz, J. V. *Chem. Phys. Lett.* **1999**, *307*, 220.

(10) Kunii, T. L.; Kuroda, H. *Theor. Chim. Acta* **1968**, *11*, 97.

(11) (a) Wesolowski, S. S.; Leininger, M. L.; Pentchev, P. N.; Schaefer, H. F. *J. Am. Chem. Soc.* **2001**, *123*, 4023. (b) Richardson, N. A.; Gu, J.; Wang, S.; Xie, Y.; Schaefer, H. F., III *J. Am. Chem. Soc.* **2004**, *126*, 4404.

(12) (a) Dolgounitcheva, O.; Zakrzewski, V. G.; Ortiz, J. V. *J. Phys. Chem. A* **1999**, *103*, 7912. (b) Morgado, C. A.; Pichugin, K. Y.; Adamowicz, L. *Phys. Chem. Chem. Phys.* **2004**, *6*, 2758.

(13) (a) Desfrancois, C.; Periquet, V.; Bouteiller, Y.; Schermann, J. P. *J. Phys. Chem. A* **1998**, *102*, 1274. (b) Hendricks, J. H.; Lyapustina, S. A.; de Clercq, H. L.; Bowen, K. H. *J. Chem. Phys.* **1998**, *108*, 8.

(14) (a) Sevilla, M. D.; Besler, B. B.; Colson, A. O. *J. Chem. Phys.* **1994**, *98*, 2215. (b) Smets, J.; Smith, D. M. A.; Elkadi, Y.; Adamowicz, L. *J. Phys. Chem. A* **1997**, *101*, 9152. (c) Periquet, V.; Moreau, A.; Carles, S.; Schermann, J. P.; Desfrancois, C. *J. Electron Spectrosc. Relat. Phenom.* **2000**, *106*, 141.

(15) (a) Colson, A. O.; Besler, B.; Sevilla, M. D. *J. Phys. Chem.* **1992**, *96*, 9787. (b) Al-Jihad, I.; Smets, J.; Adamowicz, L. *J. Phys. Chem. A* **2000**, *104*, 2994. (c) Richardson, N. A.; Wesolowski, S. S.; Schaefer, H. F., III *J. Phys. Chem. B* **2003**, *107*, 848. (d) Reynisson, J.; Steenken, S. *Phys. Chem. Chem. Phys.* **2002**, *4*, 5353. (e) Kumar, A.; et al. *J. Comput. Chem.* **2004**, *25*, 1047. (f) Santamaria, R.; Charro, E.; Zacarias, A.; Castro, M. *J. Comput. Chem.* **1999**, *20*, 511. (g) Li, X.; Cai, Z.; Sevilla, M. D. *J. Phys. Chem. A* **2002**, *106*, 9345.

(16) Richardson, N. A.; Wesolowski, S. S.; Schaefer, H. F., III. *J. Am. Chem. Soc.* **2002**, *124*, 10163.

(17) (a) Li, X.; Cai, Z.; Sevilla, M. D. *J. Phys. Chem. B* **2001**, *105*, 10115. (b) Smets, J.; Jalbout, A. F.; Adamowicz, L. *Chem. Phys. Lett.* **2001**, *342*, 342. (c) Saettel, N. J.; Wiest, O. *J. Am. Chem. Soc.* **2001**, *123*, 2693. (d) Bertran, J.; Oliva, A.; Rodriquez-Santiago, L.; Soduqe, M. *J. Am. Chem. Soc.* **1998**, *120*, 8159.

(18) Hutter, M.; Clark, T. *J. Am. Chem. Soc.* **1996**, *118*, 7574.

(19) (a) Kim, S. K.; Lee, W.; Herschbach, D. R. *J. Phys. Chem.* **1996**, *100*, 7933. (b) Hush, N. S.; Cheung, A. S. *Chem. Phys. Lett.* **1975**, *34*, 11. (c) Orlov, V. M.; Smirnow, A. N.; Varshavsky, Y. M. *Tetrahedron Lett.* **1976**, *48*, 4377. (d) Lias, S. G.; Bartmess, J. E.; Liebman, J. F.; Holmes, L. J.; Levin, R. D.; Mallard, W. G. *J. Phys. Chem. Ref. Data* **1988**, 17.

(20) The mean values taken from refs 3 and 8 (discrepancies range from 0.02 to 0.20 eV).

(21) Sarma, M. H.; Gupta, G.; Sarma, R. H. *Biochemistry* **1987**, *26*, 7707.

(22) (a) Hobza, P.; Sponer, J. *Chem. Rev.* **1999**, *99*, 3247. (b) Sponer, J.; Jurecka, P.; Hobza, P. *J. Am. Chem. Soc.* **2004**, *126*, 10142.

(23) Boys, S. F.; Bernardi, F. *Mol. Phys.* **1970**, *19*, 553.

(24) Glendening, E. D.; Reed, A. E.; Carpenter, J. E.; Weinhold, F. *Natural Bond Orbital, Version 3.0*; University of Wisconsin−Madison: Madison, WI.

(25) (a) Reed, A.; Curtiss, L. A.; Weinhold, F. *Chem. Rev.* **1988**, *88*, 899. (b) Reed, A.; Weinhold, F.; Curtiss, L. A.; Pochatko, D. *J. Chem. Phys.* **1986**, *84*, 5687. (c) Reed, A.; Weinhold, F. *J. Chem. Phys.* **1985**, *83*, 1736. (d) Reed, A.; Weinstock, R. B.; Weinhold, F. *J. Chem. Phys.* **1985**, *83*, 735.

(26) Tian, S. X. *J. Phys. Chem. B* **2004**, *118*, 20388.

(27) Frisch, M. J.; Trucks, G. W.; Schlegel, H. B.; Scuseria, G. E.; Robb, M. A.; Cheeseman, J. R.; Zakrzewski, V. G.; Montgomery, J. A. Jr.; Stratmann, R. E.; Burant, J. C.; Dapprich, S.; Millam, J. M.; Daniels, A. D.; Kudin, K. N.; Strain, M. C.; Farkas, O.; Tomasi, J.; Barone, V.; Cossi, M.; Cammi, R.; Mennucci, B.; Pomelli, C.; Adamo, C.; Clifford, S.; Ochterski, J.; Petersson, G. A.; Ayala, P. Y.; Cui, Q.; Morokuma, K.; Malick, D. K.; Rabuck, A. D.; Raghavachari, K.; Foresman, J. B.; Cioslowski, J.; Ortiz, J. V.; Baboul, A. G.; Stefanov, B. B.; Liu, G.; Liashenko, A.; Piskorz, P.; Komaromi, I.; Gomperts, R.; Martin, R. L.; Fox, D. J.; Keith, T.; Al-Laham, M. A.; Peng, C. Y.; Nanayakkara, A.; Gonzalez, C.; Challacombe, M.; Gill, P. M. W.; Johnson, B.; Chen, W.; Wong, M. W.; Andres, J. L.; Gonzalez, C.; Head-Gordon, M.; Replogle, E. S.; Pople, J. A. *GAUSSIAN 98*; Gaussian, Inc.: Pittsburgh, PA, 1998.

(28) Yanson, I. K.; Teplitsky, A. B.; Sukhodub, L. F. *Biopolymers* **1979**, *18*, 1149.